arXiv:0705.0396v3 [astro-ph] 26 Dec 2007

Phantom crossing, equation-of-state singularities, and local gravity constraints in $f(R)$ models

Luca Amendola[1] and Shinji Tsujikawa[2]
[1]*INAF/Osservatorio Astronomico di Roma, Via Frascati 33*
00040 Monte Porzio Catone (Roma), Italy
[2]*Department of Physics, Gunma National College of Technology, Gunma 371-8530, Japan*

(Dated: February 1, 2008)

We identify the class of $f(R)$ dark energy models which have a viable cosmology, i.e. a matter dominated epoch followed by a late-time acceleration. The deviation from a ΛCDM model ($f = R - \Lambda$) is quantified by the function $m = Rf_{,RR}/f_{,R}$. The matter epoch corresponds to $m(r = -1) \simeq +0$ (where $r = -Rf_{,R}/f$) while the accelerated attractor exists in the region $0 \le m < 1$. We find that the equation of state $w_{\rm DE}$ of all such "viable" $f(R)$ models exhibits two features: $w_{\rm DE}$ diverges at some redshift z_c and crosses the cosmological constant boundary ("phantom crossing") at a redshift z_b smaller than z_c. Using the observational data of Supernova Ia and Cosmic Microwave Background, we obtain the constraint $m < \mathcal{O}(0.1)$ and we find that the phantom crossing could occur at $z_b \gtrsim 1$, i.e. within reach of observations. If we add local gravity constraints, the bound on m becomes very stringent, with m several orders of magnitude smaller than unity in the region whose density is much larger than the present cosmological density. The representative models that satisfy both cosmological and local gravity constraints take the asymptotic form $m(r) = C(-r-1)^p$ with $p > 1$ as r approaches -1.

I. INTRODUCTION

Recent observations have continuously confirmed that about 70% of the present energy density of the universe consists of dark energy (DE) that leads to an accelerated expansion [1]. The simplest DE scenario consistent with observations is the ΛCDM model in which DE is identified as a cosmological constant Λ. There are many other attempts to explain the origin of DE, which can be broadly classified into two classes. The first class consists of modified gravity models in which gravity is modified from Einstein theory, whereas the second class corresponds to introducing a more or less exotic form of matter (such as a scalar field [2]) to explain the late-time acceleration. One of the main focus of current research is to find a departure from the ΛCDM model by confronting dynamical DE models with observations.

In this paper we shall study cosmological and local gravity constraints on a class of modified gravity DE models [3] whose action is a general function $f(R)$ in terms of a Ricci scalar R, i.e.,

$$S = \int {\rm d}^4x \sqrt{-g} \left[\frac{1}{2\kappa^2} f(R) + \mathcal{L}_{\rm m} + \mathcal{L}_{\rm rad} \right] , \qquad (1)$$

where $\kappa^2 = 8\pi G = 1/M_{\rm pl}^2$ while G is a bare gravitational constant and $M_{\rm pl}$ is a reduced Planck mass (see also Refs. [4, 5, 6]). Here $\mathcal{L}_{\rm m}$ and $\mathcal{L}_{\rm rad}$ are the Lagrangian densities of dust-like matter and radiation, respectively. Throughout this paper we shall focus on the metric-variational approach. See Refs. [7] for the Palatini formalism of $f(R)$ DE models.

In Ref. [8] it was shown that the models of the types $f(R) = R - \alpha/R^n$ ($n > 0$) and $f(R) = \alpha R^n$ ($n \neq 1$) do not possess a standard matter epoch because of a large coupling between gravity and dark matter, even though a late-time acceleration can be realized (see also Refs. [9, 10, 11]). Extending the analysis to general $f(R)$ cases, the paper [12] has recently clarified the conditions under which $f(R)$ DE models have a matter era followed by an accelerated expansion. However this does not necessarily mean that the models satisfying the conditions derived in [12] can be consistent with observations. In this paper we constrain $f(R)$ models that have a matter epoch prior to the acceleration from the observational data such as Supernova Ia (SNIa) and the sound horizon of Cosmic Microwave Background (CMB).

The deviation from the ΛCDM model is quantified by a variable

$$m = \frac{Rf_{,RR}}{f_{,R}} , \qquad (2)$$

where $f_{,R} \equiv {\rm d}f/{\rm d}R$ and $f_{,RR} \equiv {\rm d}^2f/{\rm d}R^2$. Note that the ΛCDM model corresponds to $m = 0$. As we will show in this paper, the quantity m can be constrained as $m < \mathcal{O}(0.1)$ throughout the matter and accelerated epochs from CMB and SNIa data. This limit still allows for interesting deviations from ΛCDM, in particular for the possibility to observe a phantom crossing and a singularity at low redshifts in the equation of state of DE. However, as we will show, local gravity constraints (LGC) give a tight bound for m very much smaller than unity in a region whose density is much larger than the present cosmological density. Although this tight constraint excludes most $f(R)$ models (or renders them indistinguishable from the ΛCDM model), those proposed recently by Hu & Sawicki [13] and Starobinsky [14], which appeared after the initial submission of this article, are still viable and can be distinguished from ΛCDM.

II. VIABLE COSMOLOGICAL TRAJECTORIES

In the flat Friedmann-Robertson-Walker background with a scale factor a, the evolution equations in the metric-variational approach are given by

$$\begin{aligned} 3FH^2 &= \kappa^2\left(\rho_{\rm m}+\rho_{\rm rad}\right)+(FR-f)/2-3H\dot{F}, \quad (3)\\ -2F\dot{H} &= \kappa^2\left[\rho_{\rm m}+(4/3)\rho_{\rm rad}\right]+\ddot{F}-H\dot{F}, \quad (4)\end{aligned}$$

where $F=\partial f/\partial R$, $H=\dot{a}/a$, $R=6(2H^2+\dot{H})$, and a dot denotes a derivative in terms of cosmic time t. Note that we study the dynamics in the positive F branch. The energy densities of a non-relativistic matter and radiation satisfy the equations

$$\dot{\rho}_{\rm m}+3H\rho_{\rm m}=0\,, \tag{5}$$

$$\dot{\rho}_{\rm rad}+4H\rho_{\rm rad}=0\,, \tag{6}$$

respectively.

In order to confront the models with SNIa observations, it is convenient to write the equations as follows

$$\begin{aligned} 3F_0H^2 &= \kappa^2(\rho_{\rm DE}+\rho_{\rm m}+\rho_{\rm rad})\,, \quad (7)\\ 2F_0\dot{H} &= -\kappa^2\left[\rho_{\rm m}+(4/3)\rho_{\rm rad}+\rho_{\rm DE}+p_{\rm DE}\right]\,, \quad (8)\end{aligned}$$

where

$$\begin{aligned} \kappa^2\rho_{\rm DE} &= (1/2)(FR-f)-3H\dot{F}+3H^2(F_0-F)\,, \quad (9)\\ \kappa^2 p_{\rm DE} &= \ddot{F}+2H\dot{F}-(1/2)(FR-f)\\ &\quad -(2\dot{H}+3H^2)(F_0-F)\,. \quad (10)\end{aligned}$$

Here the subscript "0" represents present values at the redshift $z=0$. By defining $\rho_{\rm DE}$ and $p_{\rm DE}$ in the above way, these satisfy the usual conservation equation

$$\dot{\rho}_{\rm DE}+3H(\rho_{\rm DE}+p_{\rm DE})=0\,. \tag{11}$$

Then the DE equation of state (EOS) parameter, $w_{\rm DE}\equiv p_{\rm DE}/\rho_{\rm DE}$, is directly related to the one obtained from observations [15].

Introducing the following variables

$$x_1=-\frac{\dot{F}}{HF},\ x_2=-\frac{f}{6FH^2},\ x_3=\frac{R}{6H^2},\ x_4=\frac{\kappa^2\rho_{\rm rad}}{3FH^2},$$

we obtain [12]

$$\begin{aligned} x_{1,N} &= -1-x_3-3x_2+x_1^2-x_1x_3+x_4\,, \quad (12)\\ x_{2,N} &= \frac{x_1x_3}{m}-x_2(2x_3-4-x_1)\,, \quad (13)\\ x_{3,N} &= -\frac{x_1x_3}{m}-2x_3(x_3-2)\,, \quad (14)\\ x_{4,N} &= -2x_3x_4+x_1\,x_4\,, \quad (15)\end{aligned}$$

where $N=\ln a$, $x_{i,N}={\rm d}x_i/{\rm d}N$ and

$$m = \frac{{\rm d}\log F}{{\rm d}\log R}=\frac{Rf_{,RR}}{f_{,R}}\,, \tag{16}$$

$$r = -\frac{{\rm d}\log f}{{\rm d}\log R}=-\frac{Rf_{,R}}{f}=\frac{x_3}{x_2}\,. \tag{17}$$

Deriving R as a function of r from Eq. (17), one can express m as a function of $r=x_3/x_2$ and close the above system. Notice that defining $\Omega_{\rm m}\equiv\kappa^2\rho_{\rm m}/3FH^2$ one has

$$\Omega_{\rm m}=1-x_1-x_2-x_3-x_4\,. \tag{18}$$

The DE equation of state is given by

$$w_{\rm DE}=\frac{p_{\rm DE}}{\rho_{\rm DE}}=-\frac{1}{3}\frac{2x_3-1+x_4y}{1-y(1-x_1-x_2-x_3)}\,, \tag{19}$$

where $y\equiv F/F_0$. We note that the effective equation of state of the system is given by $w_{\rm eff}=-(2x_3-1)/3$.

The analysis of the phase space has been performed in great detail in [12]. Here we summarize the main results. In the absence of radiation ($x_4=0$) we have six fixed points for the above system. A matter epoch can be realized for $m\approx 0$ and $r\approx -1$ on the critical point

$$P_M:\ (x_1,x_2,x_3)=\left(\frac{3m}{1+m},-\frac{1+4m}{2(1+m)^2},\frac{1+4m}{2(1+m)}\right),$$

which satisfies $w_{\rm eff}=-\frac{m}{1+m}$. If $m\approx +0$ and $m'(r)\equiv {\rm d}m/{\rm d}r>-1$ at $r\approx -1$ the matter era corresponds to a saddle with a damped oscillation, whereas if $m<0$ a prolonged matter period is not realized because the real part of the eigenvalues of the critical point diverges (see also [10]). Note that the radiation point also exists in the region with $m\approx 0$, which corresponds to a saddle [12]. Hence a viable cosmological trajectory starts around the radiation point with $m\approx 0$, which is followed by the matter point with $m\approx 0$.

When the trajectory passes through a standard matter era P_M with $m\approx +0$, then one sees that $\Omega_{\rm m}\approx 1$. On the other hand, the future asymptotic value of $\Omega_{\rm m}$ is always zero if the acceleration occurs (see below). Therefore the denominator of $w_{\rm DE}$, which in the absence of radiation can be written as $1-F\Omega_{\rm m}/F_0$, goes from ≈ 1 in the future to $1-F/F_0$ in the deep matter era; this shows that if F increases toward the past $1-F/F_0$ crosses zero and becomes negative and consequently $w_{\rm DE}$ passes necessarily through a singularity. We will show in the next section that this is indeed what happens.

There are two stable fixed points leading to a late-time acceleration:

(i) $P_A\ :\ (x_1,x_2,x_3)=(0,-1,2),$ (20)

(ii) $P_B\ :\ (x_1,x_2,x_3)$

$$=\left(\frac{2(1-m)}{1+2m},\frac{1-4m}{m(1+2m)},-\frac{(1-4m)(1+m)}{m(1+2m)}\right).$$

The effective EOS is given by $w_{\rm eff}=-1$ for P_A and $w_{\rm eff}=\frac{2-5m-6m^2}{3m(1+2m)}$ for P_B. The former exists on the line $r=-2$ and is stable for $0<m\leq 1$. The latter exists on the line $m(r)=-r-1$ as is the case for the point P_M. There are several ranges of m that lead to a stable acceleration, but only for $(\sqrt{3}-1)/2<m<1$ and $m'(r)<-1$ one can have a transition from the saddle matter era to the accelerated epoch (in this case $w_{\rm eff}>-1$) (see discussions in [12]). Therefore, we have only two qualitatively different viable cases:

- Models that link P_M with P_A (Class A),
- Models that link P_M with P_B (Class B).

See Fig. 1 for an illustration.

The cosmological dynamics of $f(R)$ models can be well understood by considering $m(r)$ curves in the (r, m) plane. The ΛCDM model, $f(R) = R - \Lambda$, corresponds to $m = 0$, in which case the trajectory is a straight line from P_M: $(r, m) = (-1, 0)$ to P_A: $(r, m) = (-2, 0)$. We now introduce three $f(R)$ toy models that represent the two qualitatively different classes of cosmologies A and B. As Class A we define a minimal generalization of the ΛCDM model given by (model A1)

$$f(R) = (R^b - \Lambda)^c \,. \tag{21}$$

This is characterized by the straight line

$$m(r) = [(1-c)/c]r + b - 1 \,. \tag{22}$$

The existence of a saddle matter epoch requires the condition $c \geq 1$ and $bc \approx 1$. When $c = 1$ the trajectory is given by $m = b - 1$ and is parallel to the ΛCDM line ($m = 0$). We also introduce models of the type (model A2)

$$f(R) = R - \alpha R^n \,, \quad \alpha > 0, \quad 0 < n < 1 \,, \tag{23}$$

which satisfy $m = n(1+r)/r$ and also fall into the Class A [11, 12]. As representative of Class B, i.e., a cosmological evolution from P_M to P_B, we select the models (model B1)

$$m(r) = -C(r+1)(r^2 + ar + b) \,, \tag{24}$$

where $C > 0$. We require the conditions $m'(-1) = -C(1-a+b) > -1$ and $m'(-2) = C(3a-b-8) < -1$ for the transition from the matter era to the stable acceleration. In Fig. 1 we plot four trajectories corresponding to the various cases we presented above. These toy models are meant only to exemplify the classes of viable cosmologies; it is clear that there are an infinite number of $m(r)$ curves connecting P_M to $P_{A,B}$. However, most of our arguments below will apply to any of these curves.

III. OBSERVATIONAL CONSTRAINTS

For the viability of $f(R)$ models we require that they satisfy three observational constraints: (i) CMB, (ii) SNIa and (iii) LGC. The first one comes from the angular size of the sound horizon defined by

$$\Theta_s = \int_{z_{\rm dec}}^{\infty} \frac{c_s(z){\rm d}z}{H(z)} \bigg/ \int_0^{z_{\rm dec}} \frac{{\rm d}z}{H(z)} \,, \tag{25}$$

where $c_s^2(z) = 1/[3(1+3\rho_b/4\rho_\gamma)]$ is the adiabatic baryon-photon sound speed and $z_{\rm dec} \simeq 1089$ is the redshift at the decoupling time. This quantity Θ_s is related to the position of CMB acoustic peaks and has been constrained as $\Theta_s = 0.5946 \pm 0.0021$ deg from the WMAP 3year data [16]. Since the eigenvalues of the Jacobian matrix for perturbations about the matter point P_M are given by $3(1 + m'(r))$ and $-3/4 \pm \sqrt{-1/m}$, the matter epoch ($m \approx +0$) lasts for a long time as the tangent $m'(-1)$ approaches -1. If $m'(-1)$ is close to -1 it is generally difficult to satisfy the CMB constraint.

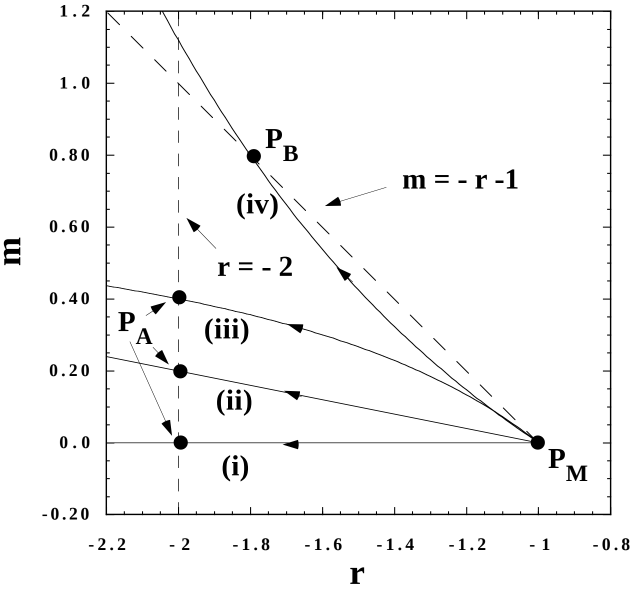

Figure 1: 4 trajectories in the (r, m) plane. Each trajectory corresponds to (i) ΛCDM, (ii) $f(R) = (R^b - \Lambda)^c$, (iii) $f(R) = R - \alpha R^n$ with $\alpha > 0, 0 < n < 1$, and (iv) $m(r) = -C(r + 1)(r^2 + ar + b)$. Here P_M, P_A and P_B are matter, de-Sitter and non-phantom accelerated points, respectively.

We have integrated the autonomous equations to obtain the present matter density $\Omega_{\rm m}^{(0)} = 0.28$. Then we solved back the equations toward the past to get $\Theta_s = 0.5946 \pm 0.0021$. This is a trial and error procedure that is done by changing initial conditions in the radiation era. If the present radiation density satisfies the condition $5.0 \times 10^{-5} < \Omega_{\rm rad}^{(0)} < 2.5 \times 10^{-4}$ together with the sound horizon constraint, we conclude that the models pass the CMB test. Then the straight line model A1 given in (21), for example, is constrained to $c < 3$ and $m < 0.282$. For larger c the contribution of dark energy is significant even in the matter-dominated epoch, thus incompatible with the CMB constraint. This comes from the fact that as m deviates from 0 the coupling between dark energy and dark matter becomes significant.

In what follows we shall consider the SNIa constraint under the situation where the CMB constraint is satisfied. The viable cosmological trajectories are restricted to be in the range $m > 0$ and $r < 0$. Since we are considering the case of positive F, this translates into the conditions $RF_{,R} > 0$ and $R/f > 0$. If R changes sign, both m and r change signs simultaneously. Then it is sufficient to consider positive R, which gives $F_{,R} > 0$. This

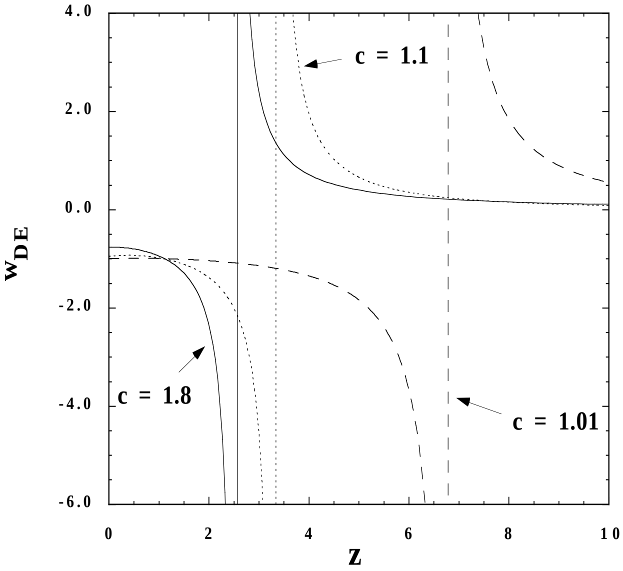

Figure 2: Evolution of the DE equation of state $w_{\rm DE}$ for the model $f(R) = (R^{1/c} - \Lambda)^c$ with parameters $c = 1.01, 1.1, 1.8$. As c approaches 1, the critical value z_c gets larger. In the limit $c \to 1$ (ΛCDM model) we have $z_c \to \infty$.

translates into the condition $\dot{F} < 0$ when R decreases in time, which means that the variable F increases toward the past. Hence the DE equation of state exhibits a divergence at some redshift $z_c > 0$ because $\rho_{\rm DE}$ changes sign. Since $p_{\rm DE}$ is negative provided $x_3 \geq 1/2$ (in which case the radiation, matter and accelerated epochs are included), we have $w_{\rm DE} < 0$ for $z < z_c$ and $w_{\rm DE} > 0$ for $z > z_c$ together with the singularity $w_{\rm DE} \to -\infty$ as $z \to -z_c$ and $w_{\rm DE} \to +\infty$ as $z \to +z_c$. [1] This shows an interesting feature of $f(R)$ models: whenever they are cosmologically acceptable they exhibit a singularity in $w_{\rm DE}$ at some epoch in the past and, as a consequence, a crossing of the "phantom boundary" $w_{\rm DE} = -1$. Note that the models with $F_{,R} < 0$ (such as $f(R) = R - \alpha/R^n$, $n > 0$) do not exhibit such peculiar behavior, but they are not cosmologically viable [8].

In Fig. 2 we plot the evolution of $w_{\rm DE}$ for the model (21) with $bc = 1$ for three different values of c. The ΛCDM model ($c = 1$) corresponds to $z_c \to \infty$. As c deviates from 1, the critical redshift z_c gets smaller together with the increase of the present value of $w_{\rm DE}$ departing from -1. The phantom crossing ($w_{\rm DE} = -1$) is realized at the redshift z_b smaller than z_c. It is worth pointing out that the phantom crossing occurs from the region $w_{\rm DE} < -1$ to the region $w_{\rm DE} > -1$, which is different from quintom models of DE [18]. In Table I we show the values z_b, z_c, $w_{\rm DE}(z=0)$ and $m(z=0)$ with several different choices of c. We find that z_b is generally close to unity (unless $w_{\rm DE}$ today is extremely close to -1), which is within the observational range of SNIa. This interesting feature could be employed to discriminate $f(R)$ modified gravity from other dark energy models. The divergence of $w_{\rm DE}$ occurs at a redshift larger than $z = 2$ (if one also imposes the CMB constraints), so this is outside of the current observational range of SNIa.

c	z_b	z_c	$w_{\rm DE}(z=0)$	$m(z=0)$
1.01	1.20	6.77	-0.996	0.008
1.1	1.09	3.33	-0.952	0.076
1.5	1.05	2.55	-0.818	0.222
1.8	1.12	2.52	-0.766	0.256
2.3	1.24	2.61	-0.705	0.276

Table I: The values of z_b, z_c, $w_{\rm DE}(z=0)$ and $m(z=0)$ for the model $f(R) = (R^{1/c} - \Lambda)^c$. The present epoch corresponds to $\Omega_{\rm m}^{(0)} = 0.28$.

Model	Constraints	z_c
$f = (R^{1/c} - \Lambda)^c$	$m < 0.276,\ c < 2.3$	2.61
$f = R - \alpha R^n\ (0 < n < 1)$	$m < 0.252,\ n < 0.7$	2.87
$m = -C(r+1)(r+2.1)$	$m < 0.151,\ C < 0.5$	2.95
$m = -C(r+1)(r^2+r+1)$	$m < 0.295,\ 1/3 < C < 0.45$	2.40

Table II: The constraint on the parameter m for several $f(R)$ models coming from the SNIa constraint $w_{\rm DE}(z=0) < -0.7$ and the CMB. We also show the value z_c corresponding to the maximum allowed m.

We can also use the criterion $w_{\rm DE}(z=0) < -0.7$ for the compatibility with the SNIa data [19]. Then in the model A1 we obtain the constraint $c < 2.3$ and $m < 0.276$, which is slightly stronger than the one obtained by the CMB. We have also carried out a numerical analysis for the other $f(R)$ models A2 and B1 described in the previous section. In Fig. 3 the evolution of m is plotted as a function of z in the marginal cases satisfying both the CMB and SNIa requirements. The constraints on m for the models (A1) $f = (R^{1/c} - \Lambda)^c$; (A2) $f = R - \alpha R^n$ $(0 < n < 1)$, and (B1) $m = -C(r+1)(r^2+r+1)$ are similar at all redshifts. Adopting instead a further model (A3) $m = -C(r+1)(r+2.1)$ (which also belongs to the class A) gives a tighter constraint near the present epoch. This is simply due to the fact that m decreases as r approaches -2 after having a maximum value of m at $r = -1.55$ in the (r, m) plane. The difference between class A and B models is not significant provided the point P_B exists in the large m region close to 1 to ensure sufficient acceleration. In Table II we summarize the maximum values of m and the allowed model parameters. As one can see, the parameter m is constrained to be $m <$ 0.1-0.3 in all models we have considered. We have also checked that the slopes of the EOS, $|{\rm d}w_{\rm DE}/{\rm d}z|$, are smaller than ≈ 0.1 at present epoch and do not provide better constraints than the ones obtained from the criterion $w_{\rm DE}(z=0) < -0.7$.

As we have seen, the cosmological observations require m to lie below 0.1-0.3 at all redshifts (up to the radiation

---

[1] We note that a divergence of $w_{\rm DE}$ can occur for a Dvali-Gabadadze-Porrati braneworld model [17].

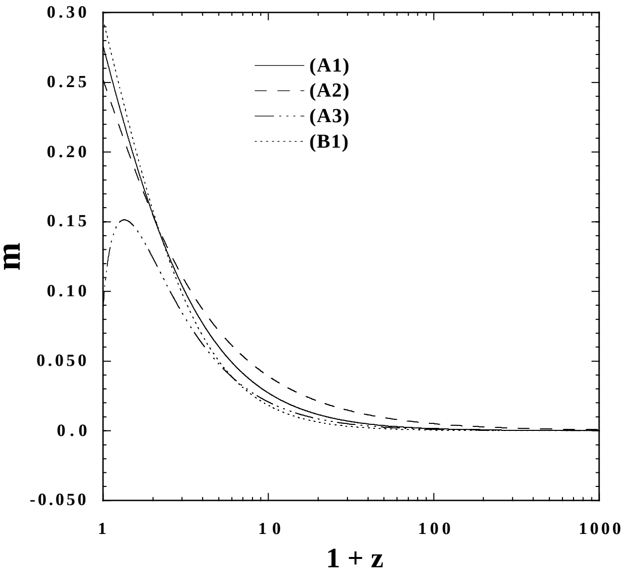

Figure 3: Evolution of the variable m in terms of z for the models: (A1) $f=(R^{1/c}-\Lambda)^c$, (A2) $f=R-\alpha R^n$ $(0<n<1)$, (A3) $m=-C(r+1)(r+2.1)$ and (B1) $m=-C(r+1)(r^2+r+1)$. Each curve shows the maximal m that still satisfies SNIa and CMB constraints.

epoch). For these values, the models display a phantom crossing and an equation of state singularity at a redshift of a few, making such $f(R)$ theories quite intriguing from the observational point of view, especially since some SN analysis finds some evidence for a similar crossing (see e.g. [20]).

Let us now include the constraints from local gravity experiments. The Newtonian effective gravitational constant can be obtained under a weak-field approximation by considering a spherically symmetric body with a mass $M_\odot$, constant density ρ and a radius $r_\odot$ and a vanishing density ($\rho=0$) outside the body. Using a linear perturbation theory in the Minkowski background with a perturbation $h_{\mu\nu}$ and decomposing the function F into background and perturbation parts ($F=F_0+\delta F$), the effective gravitational potential at a distance ℓ from the center of the body is [23, 24, 25, 26]

$$G_{\rm eff}=\frac{G}{F_0}\left(1+\frac{1}{3}e^{-M\ell}\right)\,, \tag{26}$$

where the mass M is given by

$$M^2=\frac{R}{3}\left(\frac{f_{,R}}{Rf_{,RR}}-1\right)=\frac{R}{3m}(1-m)\,, \tag{27}$$

If $M^2<0$ the Yukawa correction $e^{-M\ell}$ in Eq. (26) is replaced by an oscillating function $\cos(|M|\ell)$, but this case is excluded experimentally. Hence the mass squared is required to be positive.

As emphasized in Ref. [25], the expression (26) is valid in the regime in which the linear approximation $|\delta R|\ll R_0$ holds (here δR is a perturbation in R with R_0 being a background value). The condition for the validity of the linear approximation is given in Eq. (33) of Ref. [25], which is equivalent to

$$m(R_0)\gg\Phi_c\,, \tag{28}$$

where m is defined in Eq. (2) and $\Phi_c=GM_\odot/r_\odot$ is the gravitational potential at the surface of the body. Since the mass squared M^2 is estimated as $M^2\simeq R/3m$ for $m\ll 1$, the condition (28) tends to be violated for large M. If we require $M\ell\gg 1$ with ℓ being the scale of the experiment (e.g. a scale of 1 mm for laboratory constraints or a scale of 1 AU for solar system constraints), we obtain

$$m\ll 8\pi G_N\ell^2\rho\,, \tag{29}$$

where $G_N\equiv G/F_0$ is the gravitational constant measured at scales much larger than ℓ. Note that we used the relation $R\approx\kappa^2\rho/F_0$. This constraint is extremely stringent: assuming e.g. $\ell=1\,{\rm AU}$ and $\rho=10^{-23}\,{\rm g/cm^3}$ (corresponding to the average density in the solar system) one gets $m\ll 10^{-23}$. Similar (or stronger) values are obtained for other experimental settings on the Earth or near other solar-system bodies. Combining Eqs. (28) and (29) we see that the condition for the applicability at a distance ℓ from the center of a spherical structure of the linear perturbation approach is that

$$\ell^3\rho(\ell)\gg\int_0^\ell\rho(\ell')\ell'^2{\rm d}\ell'\,, \tag{30}$$

which, for most astrophysical bodies, is actually violated. In particular, since $\Phi_c\approx 10^{-9}\sim 10^{-6}$ for the Earth or the Sun or other planetary bodies, we find that Eq. (28) is actually grossly violated for local gravity experiments and we need to consider the non-linear regime.

When the mass M is heavy, the system enters a non-linear stage in which a thin-shell develops inside the body through a chameleon mechanism [27]. In order to consider the chameleon effect in $f(R)$ gravity, it is convenient to transform to the Einstein frame by a conformal transformation. Introducing a scalar field ϕ as $F=\exp(\sqrt{2/3}\kappa\phi)$, the potential in the Einstein frame is given by $V=(RF-f)/2\kappa^2F^2$ with a constant coupling $\beta=-1/\sqrt{6}$ between the matter and the field ϕ [8, 21].

In a spherically symmetric setting with an energy density ρ, we obtain the following equation for the field ϕ [27, 28]

$$\frac{{\rm d}^2\phi}{{\rm d}\tilde{\ell}^2}+\frac{2}{\tilde{\ell}}\frac{{\rm d}\phi}{{\rm d}\tilde{\ell}}=\frac{{\rm d}V_{\rm eff}}{{\rm d}\phi}\,, \tag{31}$$

where $\tilde{\ell}$ is the distance from the center of symmetry in the Einstein frame and

$$V_{\rm eff}(\phi)=V(\phi)+e^{\beta\kappa\phi}\rho^*\,. \tag{32}$$

The energy density ρ^* is defined by $\rho^*\equiv e^{3\beta\kappa\phi}\rho$, which is conserved in the Einstein frame [27].

Let us consider a spherically symmetric body with an energy density $\rho^* = \rho_A^*$ inside the body ($\tilde{\ell} < \tilde{r}_\odot$) and an energy density $\rho^* = \rho_B^* \ll \rho_A^*$ outside the body ($\tilde{\ell} > \tilde{r}_\odot$). Then the effective potential (32) has two minima at $\phi = \phi_A$ and $\phi = \phi_B$ satisfying the relations $V_{,\phi}(\phi_A) + \beta\kappa e^{\beta\kappa\phi_A}\rho_A^* = 0$ and $V_{,\phi}(\phi_B) + \beta\kappa e^{\beta\kappa\phi_B}\rho_B^* = 0$, respectively. The effective masses at the potential minima are defined by $m_A^2 \equiv V''_{\rm eff}(\phi_A)$ and $m_B^2 \equiv V''_{\rm eff}(\phi_B)$, where the mass m_A is much heavier than the mass m_B.

When a body has a thin shell, the solution to Eq. (31) in the region $\tilde{\ell} > \tilde{r}_\odot$ is approximately given by [26, 27, 28, 29]

$$\phi(\tilde{\ell}) \simeq -\frac{\beta_{\rm eff}}{4\pi M_{\rm pl}} \frac{M_\odot e^{-m_B(\tilde{\ell}-\tilde{r}_\odot)}}{\tilde{\ell}} + \phi_B\,, \tag{33}$$

where $M_\odot = 4\pi r_\odot^3 \rho_A/3 = 4\pi \tilde{r}_\odot^3 \rho_A^*/3$,

$$\beta_{\rm eff} = 3\beta\frac{\Delta\tilde{r}_\odot}{\tilde{r}_\odot}\,, \quad \frac{\Delta\tilde{r}_\odot}{\tilde{r}_\odot} = -\frac{\phi_B - \phi_A}{\sqrt{6}M_{\rm pl}\Phi_\odot}\,, \tag{34}$$

and $\Phi_\odot = GM_\odot/\tilde{r}_\odot$. As long as the thin-shell condition $\Delta\tilde{r}_\odot/\tilde{r}_\odot \ll 1$ is satisfied, the effective coupling $|\beta_{\rm eff}|$ becomes much smaller than unity. In this case the models can be consistent with the results of solar system experiments as well as equivalence principle experiments. For example, in the case of two identical bodies with mass M_c, the potential energy associated with the fifth force between the bodies is given by $U(\ell) = 2\beta_{\rm eff}^2 (GM_c^2/\ell)\, e^{-m_B\ell}$ [27]. The laboratory experiment constraints, $2\beta_{\rm eff}^2 < 10^{-3}$, are satisfied for $\Delta\tilde{r}_\odot/\tilde{r}_\odot \ll 1$.

In order to understand the condition under which the body has a thin shell, let us consider the model (23) with $\alpha = \lambda R_c^{1-n}$. Note that R_c is not much different from the order of the present cosmological constant. In this case the Ricci scalar R_1 at the de-Sitter point P_A satisfies the relation $\lambda = (R_1/R_c)^{1-n}/(2-n)$. In the region with a high density satisfying the relation $R \gg R_c$, the field ϕ_B and the parameter $m(R)$ are approximately given by

$$\phi_B \;\simeq\; -\frac{\sqrt{6}}{2}\lambda n \left(\frac{R_c}{\kappa^2\rho_B}\right)^{1-n} M_{\rm pl}\,, \tag{35}$$

$$m(R) \;\simeq\; \lambda n(1-n)\left(\frac{R_c}{R}\right)^{1-n}\,. \tag{36}$$

Using the fact that the Ricci scalar R_B in the region B is approximated by $R_B \simeq \kappa^2\rho_B$, we find that the thin-shell parameter is

$$\frac{\Delta\tilde{r}_\odot}{\tilde{r}_\odot} \simeq \frac{1}{2(1-n)}\frac{m(R_B)}{\Phi_\odot}\,. \tag{37}$$

This shows that, unless n is very close to 1, the thin-shell condition $\Delta\tilde{r}_\odot/\tilde{r}_\odot \ll 1$ holds for

$$m(R_B) \ll \Phi_\odot\,, \tag{38}$$

which is opposite to the condition (28) for the validity of the linear perturbation theory. When the nonlinearity becomes important the body has a thin-shell. Since $\Phi_\odot \sim 10^{-6}$ and 10^{-9} for the Sun and the Earth respectively, the condition (38) shows that the parameter m is very much smaller than unity in a high-density region where local gravity experiments are carried out ($R_B \gg R_c$).

The current tightest constraint on the post-Newtonian parameter γ in solar-system tests comes from Cassini tracking, which gives $|\gamma - 1| < 2.3 \times 10^{-5}$ [33], This translates into the bound [28]

$$\frac{\Delta\tilde{r}_\odot}{\tilde{r}_\odot} < 1.15 \times 10^{-5}\,. \tag{39}$$

Using this bound for Eq. (37) with the value $\Phi_\odot \simeq 2.12 \times 10^{-6}$ of the Sun, we obtain

$$\frac{n}{2-n}\left(\frac{\rho_1}{\rho_B}\right)^{1-n} < 4.9 \times 10^{-11}\,, \tag{40}$$

where $\rho_1 = R_1/\kappa^2$. Taking $\rho_1 = 10^{-29}$ g/cm^3 as the present cosmological density and $\rho_B = 10^{-24}$ g/cm^3 as dark and baryonic matter density in our galaxy, we obtain

$$n < 5 \times 10^{-6}\,. \tag{41}$$

Thus the model is very close to the ΛCDM model. The bound on n becomes even tighter if we take into account constraints from the equivalence principle [34].

Note that other $f(R)$ models we discussed in the previous section also need to be very close to the ΛCDM model from the LGC. In such models the parameter m behaves as $m = C(-r-1)$ as r approaches -1 (here C is a positive constant). If we demand that the present value of m is of the order of 0.1 to find a deviation from the ΛCDM model, it is generally difficult to realize very small values of m around the region $r \approx -1$ to satisfy the constraint (38).

It is also worth mentioning that the model of Ref. [35], $f(R) = R - \lambda_1 R_c \exp(-R/\lambda_2 R_c)$ with $\lambda_1, \lambda_2 > 0$, which was explicitly introduced to satisfy the LGC without fine-tuned model parameters. When $\lambda_1 \approx 1$ the model passes the LGC for $\lambda_2 < 10^4$. However, this model is not cosmologically acceptable since it does not have a late-time accelerated attractor. We find in fact applying the criteria set forth in Ref. [12] that (i) the de Sitter point P_A is not stable and (ii) the model does not have an intersection point with the line $m = -r-1$ except for the point $(r, m) = (-1, 0)$, which implies that there are no additional accelerated attractors beside the unstable de-Sitter point.

After the initial submission of this article, two viable models were independently proposed by (i) Hu & Sawicki [13] and by (ii) Starobinsky [14]:

$$\text{(i)}\quad f(R) = R - \lambda R_c \frac{(R/R_c)^{2n}}{(R/R_c)^{2n}+1}\,, \tag{42}$$

$$\text{(ii)}\quad f(R) = R - \lambda R_c \left[1 - \left(1 + R^2/R_c^2\right)^{-n}\right]\,, \tag{43}$$

where n, λ and R_c are positive constants. In such models the following relation holds in the region $R \gg R_c$ [32]:

$$m(r) \simeq C(-r-1)^{2n+1}\,, \tag{44}$$

where $C = 2n(2n+1)/\lambda^{2n}$. For larger n, $m(r)$ decreases very rapidly as r approaches -1 to satisfy the LGC. Moreover, since $m(r=-2) = C$ at the de-Sitter point P_A, it is possible to find a deviation from the ΛCDM model around the present epoch for C of the order of 0.1. The detailed analysis about these models can be found in Refs. [13, 14, 29, 32], which showed that the models can be consistent with both cosmological and local gravity constraints for $n \geq 2$. Note that the model $f(R) = R - \lambda R_c \tanh\left(R/R_c\right)$ introduced in Ref. [32] is also viable, which can be regarded as the limit $n \to \infty$ in the models (42) and (43). (see also Ref. [31] for a similar model).

IV. CONCLUSIONS

We have shown that the variable m that characterizes the deviation from the ΛCDM model is constrained to be $m < \mathcal{O}(0.1)$ from the observational data of CMB and SNIa. We find that in general the $f(R)$ models that are cosmologically acceptable exhibit a very peculiar behavior of the effective equation of state $w_{\rm DE}$: this crosses in fact the phantom boundary and undergoes a singularity at a redshift of a few. If future observations will give the precise evolution of $w_{\rm DE}$ in the high-redshift range, it could be possible to detect the peculiar features of the $f(R)$ models. This appears as an interesting way to distinguish $f(R)$ DE models from the ΛCDM cosmology.

When we consider the local gravity constraints, we find that the deviation parameter m is required to be very much smaller than unity in the high-density region where such experiments are carried out. In the $f(R)$ models we studied in Sec. II, the parameter m has asymptotic behaviour $m \propto (-r-1)$ as r approaches -1. If we demand that an appreciable deviation from the ΛCDM model can be found around the present epoch $(m(z \sim 0) = \mathcal{O}(0.1))$, we find that it is difficult to satisfy the LGC because m does not decrease very rapidly in the region with a higher density. In such models viable cosmological trajectories satisfying all these constraints are hardly distinguishable from the ΛCDM model. However, the recently proposed models (42) and (43) can exhibit a deviation from the ΛCDM around the present epoch while satisfying the LGC because the parameter m decreases rapidly in the higher-density region ($R \gg R_c$). It would be of interest to place observational constraints on such models including the data of matter power spectrum, SN Ia and weak lensing as well as LGC under the chameleon mechanism.

ACKNOWLEDGEMENTS

We thank R. Gannouji, W. Hu, B. Li, D. Polarski and A. Starobinsky for useful discussions. S. T. is supported by JSPS (Grant No. 30318802).

[1] V. Sahni and A. A. Starobinsky, Int. J. Mod. Phys. D **9**, 373 (2000); S. M. Carroll, Living Rev. Rel. **4**, 1 (2001); V. Sahni, Lect. Notes Phys. **653**, 141 (2004) [arXiv:astro-ph/0403324]; T. Padmanabhan, Phys. Rept. **380**, 235 (2003); P. J. E. Peebles and B. Ratra, Rev. Mod. Phys. **75**, 559 (2003); E. J. Copeland, M. Sami and S. Tsujikawa, Int. J. Mod. Phys. D **15**, 1753 (2006); S. Nojiri and S. D. Odintsov, Int. J. Geom. Meth. Mod. Phys. **4**, 115 (2007).

[2] Y. Fujii, Phys. Rev. D **26**, 2580 (1982); C. Wetterich, Nucl. Phys B. **302**, 668 (1988); B. Ratra and J. Peebles, Phys. Rev D **37**, 321 (1988); I. Zlatev, L. M. Wang and P. J. Steinhardt, Phys. Rev. Lett. **82**, 896 (1999).

[3] S. Capozziello, V. F. Cardone, S. Carloni and A. Troisi, Int. J. Mod. Phys. D **12**, 1969 (2003); S. M. Carroll, V. Duvvuri, M. Trodden and M. S. Turner, Phys. Rev. D 70, 043528 (2004).

[4] A. A. Starobinsky, Phys. Lett. B **91**, 99 (1980).

[5] S. Capozziello, F. Occhionero and L. Amendola, Int. J. Mod. Phys. D **1** (1993) 615.

[6] S. Nojiri and S. D. Odintsov, Phys. Rev. D **68**, 123512 (2003); A. D. Dolgov and M. Kawasaki, Phys. Lett. B **573**, 1 (2003); T. Chiba, Phys. Lett. B **575**, 1 (2003); M. E. Soussa and R. P. Woodard, Gen. Rel. Grav. **36**, 855 (2004); G. Allemandi, A. Borowiec and M. Francaviglia, Phys. Rev. D **70**, 103503 (2004); D. A. Easson, Int. J. Mod. Phys. A **19**, 5343 (2004); S. M. Carroll *et al.*, Phys. Rev. D **71**, 063513 (2005); S. Carloni, P. K. S. Dunsby, S. Capozziello and A. Troisi, Class. Quant. Grav. **22**, 4839 (2005).

[7] D. N. Vollick, Phys. Rev. D **68**, 063510 (2003); X. Meng and P. Wang, Class. Quant. Grav. **20**, 4949 (2003); E. E. Flanagan, Phys. Rev. Lett. **92**, 071101 (2004); S. Nojiri and S. D. Odintsov, Gen. Rel. Grav. **36**, 1765 (2004); T. P. Sotiriou, Class. Quant. Grav. **23**, 1253 (2006); M. Amarzguioui, O. Elgaroy, D. F. Mota and T. Multamaki, Astron. Astrophys. **454**, 707 (2006); N. J. Poplawski, Phys. Rev. D **74**, 084032 (2006); B. Li and M. C. Chu, Phys. Rev. D **74**, 104010 (2006); G. J. Olmo, Phys. Rev. Lett. **98**, 061101 (2007); S. Fay, R. Tavakol and S. Tsujikawa, Phys. Rev. D **75**, 063509 (2007).

[8] L. Amendola, D. Polarski and S. Tsujikawa, Phys. Rev. Lett. **98**, 131302 (2007).

[9] T. Clifton and J. D. Barrow, Phys. Rev. D **72**, 103005 (2005); S. Capozziello, S. Nojiri, S. D. Odintsov and A. Troisi, Phys. Lett. B **639**, 135 (2006); L. Amendola, D. Polarski and S. Tsujikawa, arXiv:astro-ph/0605384; A. W. Brookfield, C. van de Bruck and L. M. H. Hall, Phys. Rev. D **74**, 064028 (2006); S. Nojiri and S. D. Odintsov, Phys. Rev. D **74**, 086005 (2006); V. Faraoni, Phys. Rev. D **74**, 104017 (2006);

A. Borowiec, W. Godlowski and M. Szydlowski, Phys. Rev. D **74**, 043502 (2006); S. M. Carroll, I. Sawicki, A. Silvestri and M. Trodden, New J. Phys. **8**, 323 (2006); A. de la Cruz-Dombriz and A. Dobado, Phys. Rev. D **74**, 087501 (2006); R. Bean, D. Bernat, L. Pogosian, A. Silvestri and M. Trodden, Phys. Rev. D **75**, 064020 (2007); I. Navarro and K. Van Acoleyen, JCAP **0702**, 022 (2007); T. P. Sotiriou, Phys. Lett. B **645**, 389 (2007); T. P. Sotiriou and S. Liberati, Annals Phys. **322**, 935 (2007); V. Faraoni and S. Nadeau, Phys. Rev. D **75**, 023501 (2007); D. Huterer and E. V. Linder, Phys. Rev. D **75**, 023519 (2007); S. Tsujikawa, Phys. Rev. D **76**, 023514 (2007); E. O. Kahya and V. K. Onemli, arXiv:gr-qc/0612026; M. Fairbairn and S. Rydbeck, arXiv:astro-ph/0701900; G. Cognola, M. Gastaldi and S. Zerbini, arXiv:gr-qc/0701138; D. Bazeia, B. Carneiro da Cunha, R. Menezes and A. Y. Petrov, arXiv:hep-th/0701106; T. Rador, arXiv:hep-th/0701267; L. M. Sokolowski, arXiv:gr-qc/0702097; S. Fay, S. Nesseris and L. Perivolaropoulos, arXiv:gr-qc/0703006; S. Nojiri, S. D. Odintsov and P. V. Tretyakov, arXiv:0704.2520 [hep-th]; O. Bertolami, C. G. Boehmer, T. Harko and F. S. N. Lobo, arXiv:0704.1733 [gr-qc].

[10] Y. S. Song, W. Hu and I. Sawicki, Phys. Rev. D **75**, 044004 (2007); I. Sawicki and W. Hu, Phys. Rev. D **75**, 127502 (2007).

[11] B. Li and J. D. Barrow, Phys. Rev. D **75**, 084010 (2007).

[12] L. Amendola, R. Gannouji, D. Polarski and S. Tsujikawa, Phys. Rev. D **75**, 083504 (2007).

[13] W. Hu and I. Sawicki, Phys. Rev. D **76**, 064004 (2007).

[14] A. A. Starobinsky, JETP Lett. **86**, 157 (2007).

[15] G. Esposito-Farese and D. Polarski, Phys. Rev. D **63**, 063504 (2001); B. Boisseau, G. Esposito-Farese, D. Polarski and A. A. Starobinsky, Phys. Rev. Lett. **85**, 2236 (2000); R. Gannouji, D. Polarski, A. Ranquet and A. A. Starobinsky, JCAP **0609**, 016 (2006).

[16] D. N. Spergel *et al.* [WMAP Collaboration], Astrophys. J. Suppl. **170**, 377 (2007).

[17] U. Alam and V. Sahni, Phys. Rev. D **73**, 084024 (2006).

[18] B. Feng, X. L. Wang and X. M. Zhang, Phys. Lett. B **607**, 35 (2005); Z. K. Guo, Y. S. Piao, X. M. Zhang and Y. Z. Zhang, Phys. Lett. B **608**, 177 (2005).

[19] P. Astier *et al.*, Astron. Astrophys. **447**, 31 (2006).

[20] S. Nesseris and L. Perivolaropoulos, JCAP **0701**, 018 (2007); Phys. Rev. D **75**, 023517 (2007).

[21] K. i. Maeda, Phys. Rev. D **39**, 3159 (1989).

[22] C. D. Hoyle, D. J. Kapner, B. R. Heckel, E. G. Adelberger, J. H. Gundlach, U. Schmidt and H. E. Swanson, Phys. Rev. D **70** (2004) 042004.

[23] L. Amendola, Phys. Rev. D**69**:103524 (2004).

[24] G. J. Olmo, Phys. Rev. D **72**, 083505 (2005).

[25] T. Chiba, T. L. Smith and A. L. Erickcek, Phys. Rev. D **75**, 124014 (2007).

[26] I. Navarro and K. Van Acoleyen, JCAP **0702**, 022 (2007).

[27] J. Khoury and A. Weltman, Phys. Rev. Lett. **93**, 171104 (2004); J. Khoury and A. Weltman, Phys. Rev. D **69**, 044026 (2004).

[28] T. Faulkner, M. Tegmark, E. F. Bunn and Y. Mao, Phys. Rev. D **76**, 063505 (2007).

[29] S. Tsujikawa, K. Uddin and R. Tavakol, arXiv:0712.0082 [astro-ph].

[30] G. J. Olmo, Phys. Rev. Lett. **95**, 261102 (2005); A. L. Erickcek, T. L. Smith and M. Kamionkowski, Phys. Rev. D **74**, 121501 (2006); V. Faraoni, Phys. Rev. D **74**, 023529 (2006); A. F. Zakharov, A. A. Nucita, F. De Paolis and G. Ingrosso, Phys. Rev. D **74**, 107101 (2006); G. Allemandi and M. L. Ruggiero, arXiv:astro-ph/0610661; X. H. Jin, D. J. Liu and X. Z. Li, arXiv:astro-ph/0610854; P. J. Zhang, arXiv:astro-ph/0701662.

[31] S. A. Appleby and R. A. Battye, Phys. Lett. B **654**, 7 (2007).

[32] S. Tsujikawa, arXiv:0709.1391 [astro-ph], `Physical Review D to appear (2008).`

[33] C. M. Will, Living Rev. Relativity **9** (2006), arXiv:gr-qc/0510072.

[34] S. Capozziello and S. Tsujikawa, arXiv:0712.2268 [gr-qc].

[35] P. Zhang, Phys. Rev. D **73**, 123504 (2006).